5

Resonance and Nonlinear Seismo-Acoustic Land Mine Detection

Dimitri M. Donskoy
Stevens Institute of Technology
USA

1. Introduction

Since WWII acoustic echo-location method utilized in sonars has been one of the primary approaches for detecting underwater mines. However, earlier attempts to replicate sonar approach and its modifications for detection of landmines were not successful. For example, Caulfield, 1989, House & Pape, 1994, Don & Rogers, 1994 suggested the use of acoustic impulse reflection from soil. A buried object is detected by measuring a relative change in acoustic reflectivity of soil. However, compared to water, soil is an extremely inhomogeneous medium exhibiting wide variations in the physical properties: density, porosity, moisture content, etc. These variations often have a spatial scale comparable with the size of a mine creating respective variations in acoustic reflectivity regardless of presence of buried mines. Another significant drawback of these methods is their inability to discriminate mine from clatter with similar acoustic reflectivity (rocks, tree roots, etc.) The breakthrough in acoustic landmine detection had occurred with the discovery of landmine's resonance and nonlinear behaviors.

In 1999 Sabatier and Xiang reported the results of the first field test detecting live buried landmines using seismo-acoustic approach, proposed a decade earlier (according to the patent filing date) by Sabatier & Gilbert, 2000. Sabatier & Xiang used Laser Doppler Vibrometer (LDV) to measure vibration of soil excited with an airborne sound. Fig. 1 illustrates the detection approach and the resulting image of soil vibration above a buried mine. They observed noticeable deference (contrast) in soil vibration velocities measured above and off a buried mine. The contrast was observed for a variety of antitank (AT) mines in the relatively low frequency range of 50 to 300 Hz, which was quite puzzling at the time.

Simultaneously, Scott et al., 1998, initiated a laboratory testing of the detection scheme using seismic waves and radar vibrometer. Using sophisticated signal processing, the authors demonstrated that a buried object like a mine reflects a portion of seismic energy propagating along soil surface. They suggested to utilize this reflection effect for landmine detection.

Source: Humanitarian Demining: Innovative Solutions and the Challenges of Technology, Book edited by: Maki K. Habib, ISBN 978-3-902613-11-0, pp. 392, February 2008, I-Tech Education and Publishing, Vienna, Austria

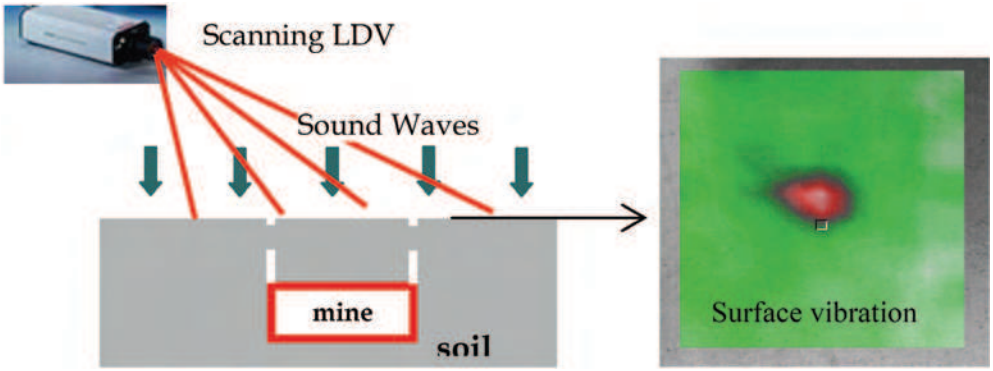

Fig. 1. Seismo-acoustic detection scheme (left) and typical vibration image of a buried mine

In the same year, Donskoy, 1998, reported first laboratory experiments demonstrating strong nonlinear dynamic behavior of buried landmines in the low frequency range below 1000 Hz. Using the same detection scheme shown in Fig. 1, Donskoy used dual harmonic excitation of soil applying airborne acoustic as well as directly coupled seismic waves and measuring nonlinear vibrations (harmonics, sum and difference frequencies) of soil above the buried mine. He noticed that the nonlinear effect is frequency dependent indicating some resonance behavior. In the following year, Donskoy, 1999, proposed a simple mass-spring model of a coupled soil-mine system explaining its resonance and nonlinear dynamics. According to this model, the combination of masses and springs (representing soil and mine dynamic stiffnesses and inertia) creates a resonance vibration response, while the nonlinearity is explained by lack of the tensile stress at the interface between a mine top surface and soil. The nonlinear mass-spring model was later refined to account for mine's own resonances and the shear stiffness of the soil column, Donskoy, et al. 2001; 2002. Further refinements included quadratic and cubic nonlinearities, Donskoy, et al., 2005 and multiple mine resonances, Zagrai, et al, 2005.

Along with the development of the nonlinear mass-spring model, the discovery of the mine's resonances was one of the key steps in understanding and developing seismo-acoustic landmine detection techniques. In 2000, our team at Stevens Institute of Technology conducted dynamic impedance measurements of over 50 live antitank (AT) and antipersonnel (AP) mines. This collection, shown in part in Fig.2, included metal, plastic, and wooden mines manufactured in different countries in Europe and Asia, as well as in the United Stated.

Fig. 2. Collection of live mines and experimental setup for dynamic impedance measurements of mines at U.S.Army testing ground

Remarkably, almost all tested mines exhibited well defined resonances with Q-factors ranging from 5 to 25 in quite narrow frequency bands: 200 Hz – 400 Hz for AT mines and 250Hz – 520 Hz for AP mines. Using this data and the model, it was possible to explain various phenomena observed during the laboratory and field measurements: high on/off mine vibration contrast (detection contrast) in the narrow frequency band observed by Sabatier & Xiang, 1999; mine's resonance responce to seismic waves, Schroeder & Scott, 2001; variation of detection frequencies and contrast level with burial depth, Sabatier, et al., 2002, Fenneman, et al ., 2003, Zagrai, et al., 2004; low detection contrast for non-mine objects such as rocks, Donskoy, et al., 2001, Schroeder & Scott, 2001; effects of moisture, temperature, and soil consolidation, Donskoy, et al., 2002.

In parallel to investigation of the mine-soil resonance behavior, our team at SIT conducted an extensive study of the nonlinear dynamics of the coupled soil-mine system. These studies, supported by numerous laboratory and field tests, demonstrated high potential of the nonlinear technique for landmine detection (Donskoy, et.al. 2002, 2005, Korman & Sabatier, 2004). Specifically, the nonlinear technique demonstrated very high (up to 40dB) detection contrast and low false alarm rate due to low clutter sensitivity.

Following this introduction, we describe major results obtained and methodology developed by the SIT team.

2. Resonance Vibrations of Land Mines

Seismo-acoustic detection of buried landmines explores the dynamic mechanical behavior of mines coupled with soil. Therefore, knowing mine's dynamic properties would be a natural first step toward understanding the mechanism of the detection, building its physical model, and developing effective detection algorithms.

In August 2000, at the U.S.Army testing site, we conducted first comprehensive measurements of variety of live mines: mines with explosive charges but without fuses. Overall over 50 mines were tested including metal, plastic and wooden AT and AP mines manufactured throughout the world. These tests involved the evaluation of mine's mechanical impedance in the frequency range 30 – 800 Hz by measuring the acoustic pressure, exerted on mine, and the resulting vibration velocity of the mine top surface. Each tested mine was placed on 2x2x2 cu. ft. concrete foundation flush buried in the ground. External force (airborne acoustic pressure) was applied with a loudspeaker suspended above the mine. We used sinusoidal signal linearly swept from 30 to 800 Hz. The acoustic pressure, P, was measured with a microphone positioned a few mm above the mine top. The mine's vibration velocity, V, was simultaneously measured just beneath the microphone using a non-contact Laser-Doppler Vibrometer. Data from the microphone and the LDV were fed into a two-channel data acquisition system which calculated and recorded magnitudes of the mine dynamic impedance (per unit area) as function of frequency, ω; $Z_m(\omega) = P(\omega)/V(\omega)$. The measurements were taken for two representative mines of the same kind and demonstrated good data repeatability. Fig. 3 presents the recorded impedances of some plastic and metal AT and AP mines. The minimum value of the impedance corresponds to the resonance frequency.

As evident from Fig.3, AT and AP mines exhibit the resonance behaviour. In fact, almost all tested mines have at least one clearly defined resonance, Table 1:

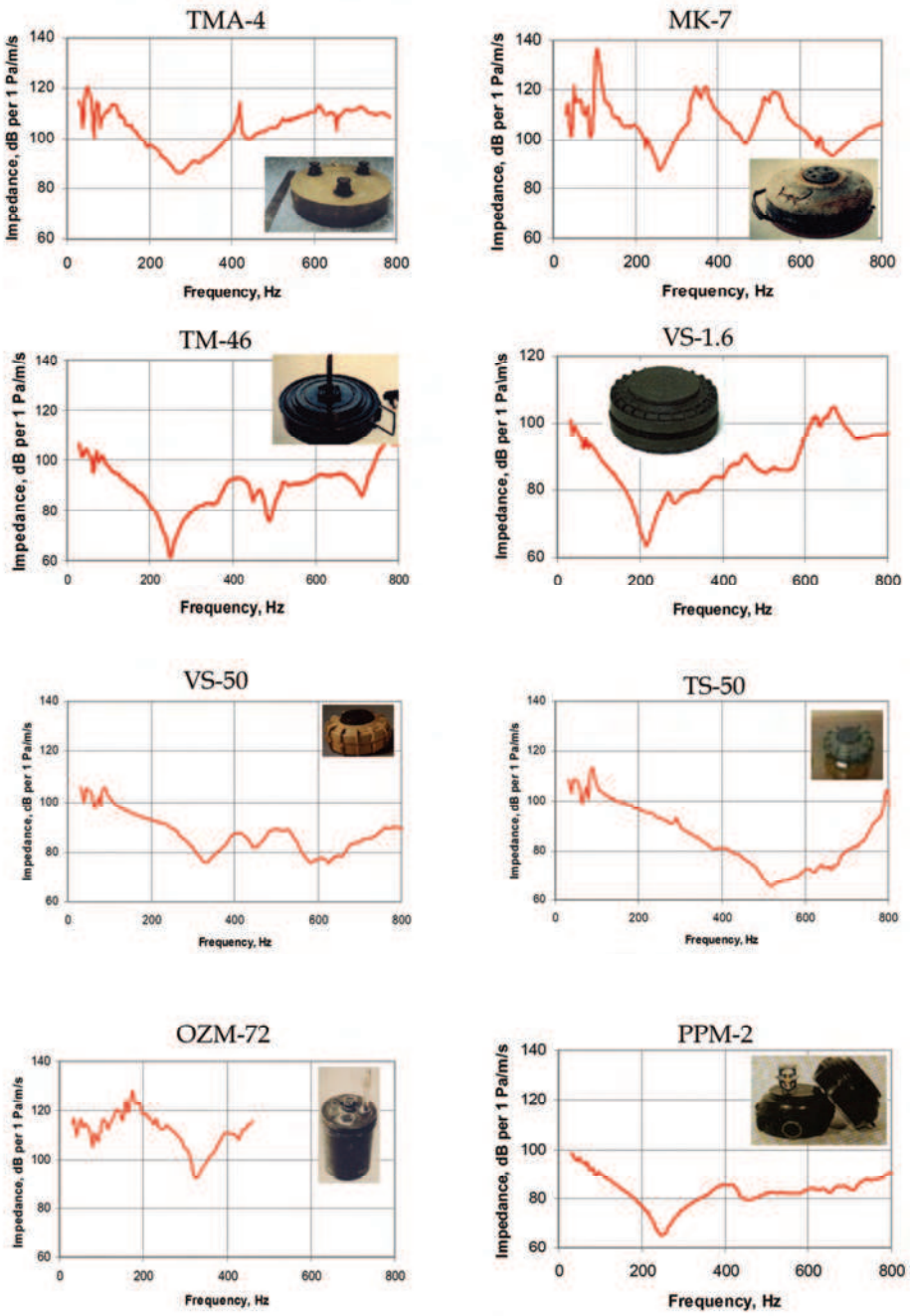

Fig. 3. Representative impedances of AT mines (TMA-4, MK-7, TM-46, VS-1.6) and AP mines (VS-50, TS-50, OZM-72, PPM-2)

Mine type	First Resonance frequency f_0 (Hz)	Dynamic stiffness K_m*10^{-7} (Pa/m)	Dynamic mass M_m (kg/m^2)	Damping constant R_m (kg/s*m^2)	Description
TS-50	520	10	9	4000	AP Plastic
VS-50	330	6	13	3300	AP Plastic
PONZ-2	380	50	85	26000	AP Plastic
PPM-2	320	4	10	4000	AP Plastic
OZM-72	330	80	190	18000	AP Metal
VS-1.6	220	2.5	12	1700	AT Plastic
TMA-5	190	0.2	1.4	300	AT Plastic
SH-55	280	2.5	8	3000	AT Plastic
VS-HCT-2	465	2.8	3.3	500	AT Plastic
TM-62P3	200	7	45	9000	AT Plastic
PTMIBA-3	260	2.5	10	1300	AT Plastic
TMA-4	250	17	65	20000	AT Metal
TM-46	250	4	16	1200	AT Metal
AT-72	200	2	14	1800	AT Wood

Table 1. Dynamic parameters of live mines

Considering a mine as an oscillator, its impedance in the vicinity of the first (lowest) resonance can be expressed through oscillator's dynamic parameters (per unit area): inertia or mass, M_m, stiffness, K_m, and damping, R_m, as following

$$z_m(\omega) = R_m + j(\omega M_m - K_m/\omega) . \quad (1)$$

Using curve fitting of the calculated impedance (1) into the measured impedance curve, we estimate the dynamic parameters of each mine for their lowest resonance. These values are also shown in Table 1.

What is the physical nature of these resonances? Depending on mine's structure, there are two major types of resonances: piston and flexural (bending) resonances of mines' upper diaphragms. Some mines, such as VS-2.2, VS-1.6, SH-55, TS-50, VS-50, and some others have a very softly supported disk-shaped pressure plate (piston). For such mines, the support is much softer than the rigidity of the plate, so the plate vibrates as a whole (as a piston) up and down or wobble from side to side or from one side only without deformation, Fig.4. These images obtained with a scanning LDV show the vibration velocity distribution at the top of the mine. The color indicates the magnitude of the velocity: red is high and green is low. Each mode is associated with the particular resonance frequency, as shown for the mine VS-50.

Many mines have a top cover rigidly connected to their side casings as it can be seen on the pictures of mines TMA-4, TM-46, MK-7, OZM-72 (Fig.3). These covers can be considered as

dynamically flexible diaphragms with the respective flexural resonating modes, example of which is depicted in Fig.5 for AT mine TMA-2.

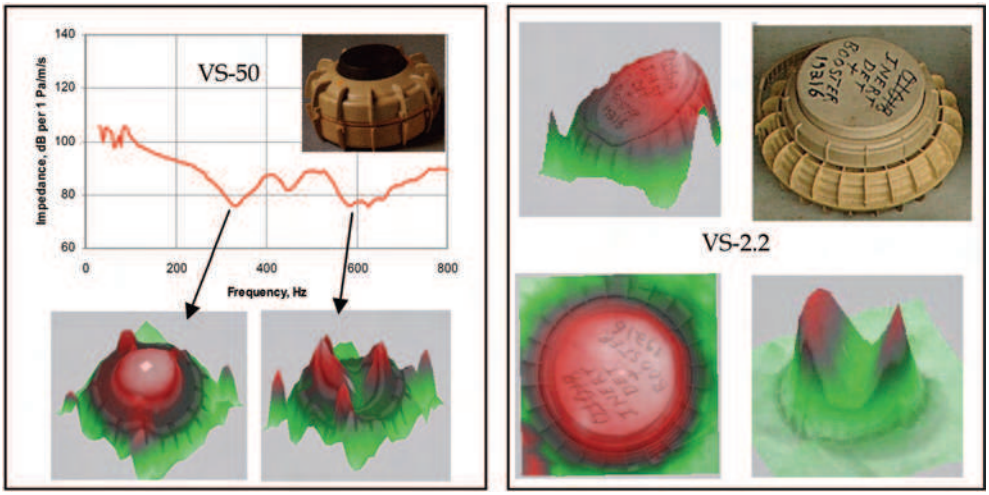

Fig. 4. Piston modes of vibration of AP mine VS-50 (left) and AT mine VS2.2 (right)

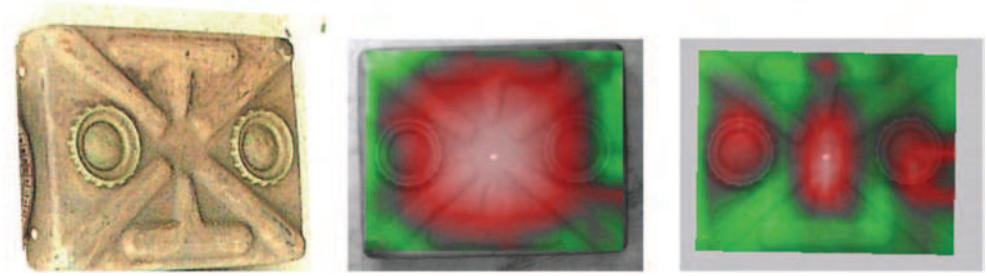

Fig. 5. Flexural modes of vibration of AT mine TMA-2 with the respective resonance frequencies 190 Hz and 490 Hz

As an example, we estimate the first flexural resonance frequency for a metal AT mine, similar to TM-46. We simplify its upper diaphragm as a clamped circular plate. The first flexural resonance frequency of this plate can be evaluated using the following formula, Skudrzyk, 1968:

$$f_0 \cong \frac{\pi h}{2R^2}\sqrt{\frac{E}{12(1-\upsilon^2)\rho}}, \tag{2}$$

where h and R are the thickness and the radius of the plate respectively and E, ν, ρ are the material parameters of the plate (Young's modulus, Poisson's ratio, and density). Thus, for 1 mm thick and 0.1 m radius steel plate, the resonance frequency is app. 240 Hz, which is a quite accurate estimate of the measured resonance frequency 250Hz for this mine.

It should be pointed out that mines exhibit not just one but multiple resonances. Although for many mines the first resonance has the lowest impedance, the higher frequency modes may also contribute to a measured soil-mine vibration response.

3. Lump-element Linear Model of Coupled Soil-mine System

One of the critical elements in understanding, developing, and implementing the mine detection technique is an adequate physical model describing dynamic behavior of the soil-mine system. The appropriate model helps to develop optimum detection algorithms and evaluate detection capabilities of the technique applied to various mine types, burial depths, and soil conditions.

The first step in developing a physical model of a dynamic system starts with a comparison of the wavelength and characteristic geometric sizes of the system. If the wavelength is shorter than the characteristic sizes, the wave approach should be used. In the opposite situation, the lump-element approach is more appropriate. In the case of a soil-mine system, the use of the lump-element (mass-spring-dashpot) approach is justified as long as low frequency waves are used: i.e. the wavelengths are greater than the size of a mine and its burial depth (characteristic sizes). The typical sizes of anti-personnel (AP) mines are in the range of 5 – 10 cm and their burial depths are up to 5 cm. The typical sizes of anti-tank (AT) mines are in the range of 20 – 30 cm and their burial depths are up to 20 cm. Wavelengths in soil depend on soil characteristics. Typically, the wavelengths are greater than 30 cm in the frequency range of hundreds of Hz: the range where the most successful practical results were obtained.

When soil is excited with acoustic or seismic waves, it vibrates directly above a buried mine with a greater amplitude than the surrounding soil. It is, in fact, one of the primary detection criteria. This suggests that some important (for detection) dynamic effects are taking place within a soil column supported by a low impedance mine (as shown in the previous section). Obviously, the mine influences the dynamics of the supported soil column; therefore, soil and mine must be treated as a dynamically coupled soil-mine system.

We start constructing the model using the Free Body Diagram (FBD) of the body of interest: mine and soil column on the top of it. Because we are interested in a perpendicular to soil surface (normal) component of vibration, in the model we account only for a normal component of the externally exerted force (normal stress σ_{zz}). The effect of the cut off from the FBD surrounding soil is represented with the shear stress, τ_{nz}, applied to the soil column around its side (cut off) surface, as shown in Fig.6.

Next, we construct a mechanical diagram (Fig.7) of the obtained FBD. The mine (rather the mine's top diaphragm responsive to the soil column vibration) is represented by its mass (inertia), M_m, compression stiffness, K_m, and damping, R_m. Similarly, dynamic properties of the soil column are described by soil inertia, M_S, compression stiffness, K_{S2} , and damping associated with the soil compression, R_{S2}. The resisting shear stress, τ_{nz} , is proportional to the soil shear modulus and shear strain and could be represented by soil shear resistance (stiffness), K_{S1}. We also add an additional damping, R_{S1}, associated with soil shear deformation.

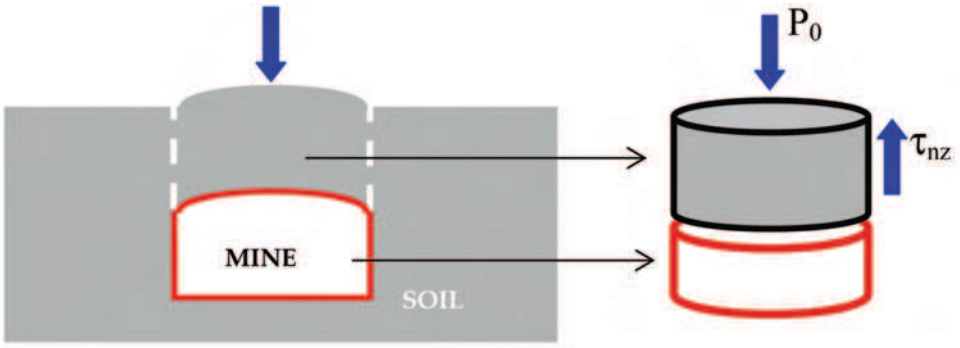

Fig. 6. Free Body Diagram (right) of vibrating mine and soil column on top of it

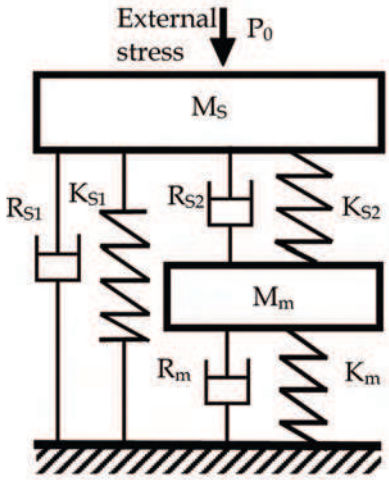

Fig.7. Linear mass-spring model of coupled soil-mine system

The introduced soil parameters are depth-dependent. The following formulas can be used to evaluate these parameters:

$$M_S \cong \rho A H \,, \tag{3}$$

where H is the burial depth, A is the effective area of the upper compliant diaphragm of the mine, and ρ is the density of the soil. The shear and compression stiffnesses, K_{S1} and K_{S2}, of the soil can be evaluated from the soil effective shear modulus, *G*, and compressibility, *B*, (Mitchell, 1993) by evaluating total shear and compressive forces acting on the vibrating soil column above the compliant mine diaphragm. For evaluation purpose we use a uniform cylindrical soil column on the top of a circular mine diaphragm having radius R. The column is under the normal stress, σ_{zz}, and its side surface is under the shear stress, τ_{nz}.

Spring stiffnesses are defined as a ratio of an exerted external force (stress) to the resulting deformation:

$$K_{S2} = (P_0 A)/\Delta_n, \quad K_{S1} = (\tau_{nz} S)/\Delta_s, \tag{4}$$

where $S = 2\pi RH$ is the side area of the column, $A = \pi R^2$ is the area of the column foundation, $\Delta_n = \varepsilon H$ and $\Delta_s = \gamma(\lambda_S/4)$ are normal and shear deformations, respectively, and λ_S is the shear wavelength. Here the deformations are defined using respective normal and shear strains, ε and γ, multiplied by respective characteristic lengths. In dynamic (wave) problems, the characteristic lengths could be estimated as a quarter of the wavelengths: compression (P-wave) wavelength for the normal deformation and shear (S-wave) wavelength for the shear deformation. In the outlined problem, however, the height of the column, H, is much less than the wavelength of the P-wave, so H is used as a characteristic length for the normal deformation. Substituting the defined deformations into the Eq.(4) and taking into account the stress-strain relationships for the normal and shear deformations, the effective soil column stiffnesses can be evaluated as

$$K_{S2} \cong A/BH, \qquad K_{S1} \cong (8\pi/\lambda_S)\, GRH, \tag{5}$$

The soil damping factors, R_{S1} and R_{S2}, are both proportional to the depth, H. (In a later study by Zagrai, et.al., 2005, the dependence for K_{S1} was modified to be proportional to H^3). The actual values of the damping coefficients could vary in a wide range depending on a soil type and conditions.

Analysis of this system is easy to perform using an equivalent electrical diagram in which external force (stress), P_0, is equivalent to voltage generator; masses, stiffnesses, and damping parameters are represented by inductances, M, capacitances, 1/K, and resistances, R, as shown in the Fig.8.

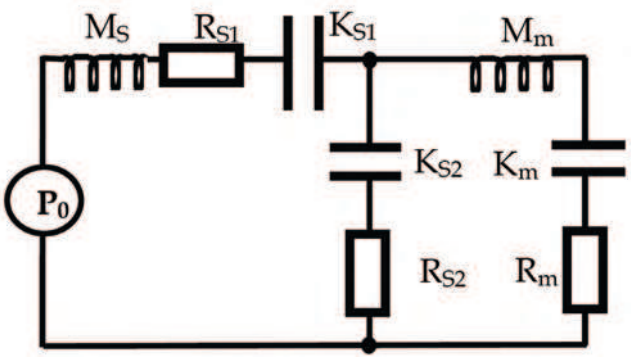

Fig.8. Equivalent electrical diagram of the mine-soil mechanical system

Using this equivalent circuit, it is easy to derive the equation for the input impedance of the soil-mine system:

$$z(\omega) = P(\omega)/V(\omega) = z_{S1} + z_{\Sigma}\,, \tag{6}$$

where

$$z_\Sigma = z_{S2}\, z_m / (z_{S2} + z_m),\ z_{S1} = R_{S1} + j(\omega M_S - K_{S1}/\omega),\ z_{S2} = R_{s2} - jK_{S2}/\omega\ , \qquad (6a)$$

and z_m is defined by the Eq.(1).
The described model is one-dimentional or single degree of freedom (SDOF). It is simple, yet very effective and easy to analyze. It explains the linear detection contrast as well as many other experimental observations, such as frequency, phase, and amplitude dependencies of the measured soil vibration as a function of various mine and soil parameters.
This SDOF model could be expanded into two-dimensional one, as it is done in Zagrai, et al, 2005, and to include the nonlinear behavior of mines, Donskoy, et al., 2002; 2005.

4. Linear Detection Contrast and its Dependence on Mine and Soil Parameters

Linear detection of buried landmines is based on measuring the ratio or difference (using dB scale) between the soil surface normal vibration velocities above and off buried mine: the linear detection contrast. This approach was initially developed and actively pursued by Sabatier and his team at the University of Mississippi (Sabatier & Xiang, 1999 and many other following publications). During their first field test with live mines, the highest detection contrast was observed in the quite narrow frequency band of 50 Hz to 300 Hz. Their theory at the time was that the detection is due to difference in porosity between highly porous soil and non-porous mines. This theory, however, could not explain the observed strong frequency dependence of the detection contrast.

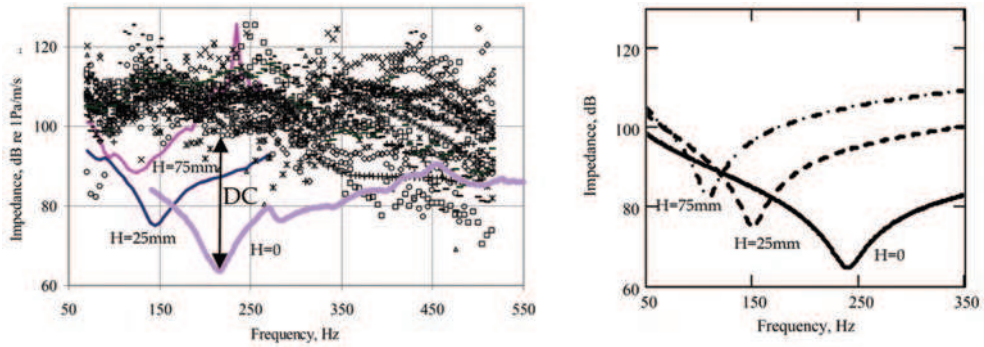

Fig. 9. Measured (left) and calculated (right) impedances of AT mine VS1.6 buried at 0, 25, and 75mm depths. Left figure also shows soil impedances measured at 23 off-mine locations at the same site. The difference between mine and soil impedances (double-sided arrow on the left) is the detection contrast (DC)

The developed lump-element model along with the evaluation of the mine's dynamic parameters provided not just qualitative, but quantitative explanation of this and other experimental observations. The model shows that the vibration response of the soil above buried mines will be resonance-like with the central (resonance) frequency determined by

the mine and soil dynamic parameters introduced in the model. Fig.8 (left) shows the impedances of soil measured at 23 off-mine locations (dotted lines) and impedances on the top and above an AT mine VS1.6 at the depths of 0 mm (flash buried), 25 mm, and 75 mm (solid lines). It demonstrates that the detection contrast is resonance-like, its maximum is depth dependant, and it diminishes with the depth. All of these are predicted by the model, Fig.9 (right).

The model explains many other field observations. For example, zero linear detection contrast (no detection) for mines buried in frozen soil, in which the shear stiffness, $K_{S2,}$ is very high. As can be seen from the model diagrams depicted in Fig.6 or Fig.7, high value of the shear stiffness dominates the total impedance of the system overwhelming the mine's contribution. Similarly, an increase in shear stiffness of consolidating soil explains the diminishing contrast for mines buried for a long period of time.

Furthermore, the analysis of the model shows that the soil shear stiffness, K_{S1}, is one of the key parameters determining the detection contrast: the higher is the stiffness, the lower is the contrast.

4.1 Effect of Soil Shear Stiffness on the Detection Contrast

A range of factors influences the detection contrast including the soil mechanical loading, its inhomogeneity, the distribution of moisture in the soil, vegetation, weathering, etc. As a result, the soil layer above the buried mine considerably affects the system dynamic response, the detection contrast, and its resonance frequency. At greater depths, the contrast is diminishing (Fig. 9) leading to poor detection and discrimination.

Understanding physical mechanisms that contribute to the reduction in soil vibration amplitude above buried mine is crucially important, since the amplitude is a key parameter used for detection. Certainly, dissipation of the elastic energy in a soil column above the mine plays an important role. However, the dissipation along can't explain the reduction of the detection contrast with time (for the same undisturbed mine) as soil consolidates. The dissipation can't account for significant contrast reduction for deeper buried mines.

Based on the model analysis, we suggest that increasing shear stiffness of soil contributes to reduction of the vibration amplitude above the buried mine. This effect is illustrated in Fig. 10, showing calculated admittances (inverse impedances) for the AT mine VS-1.6. The solid line in the figure is the admittance of the flush-buried mine (zero depth) obtained by using the experimental data from the Table 1. The dotted line represents the admittance of the mine buried at 1 cm, where $K_{S1}=2\cdot10^6$ Pa/m. Then, without modifying other parameters in the model, we calculated admittances for the higher shear stiffness: $K_{S1}=7\cdot10^7$ Pa/m (dashed line) and $K_{S1}=1.2\cdot10^8$ Pa/m (dashed-dotted line). As it could be seen from the figure, the vibration amplitude of the mine buried in the stiffer soil decreased substantially without any change in damping.

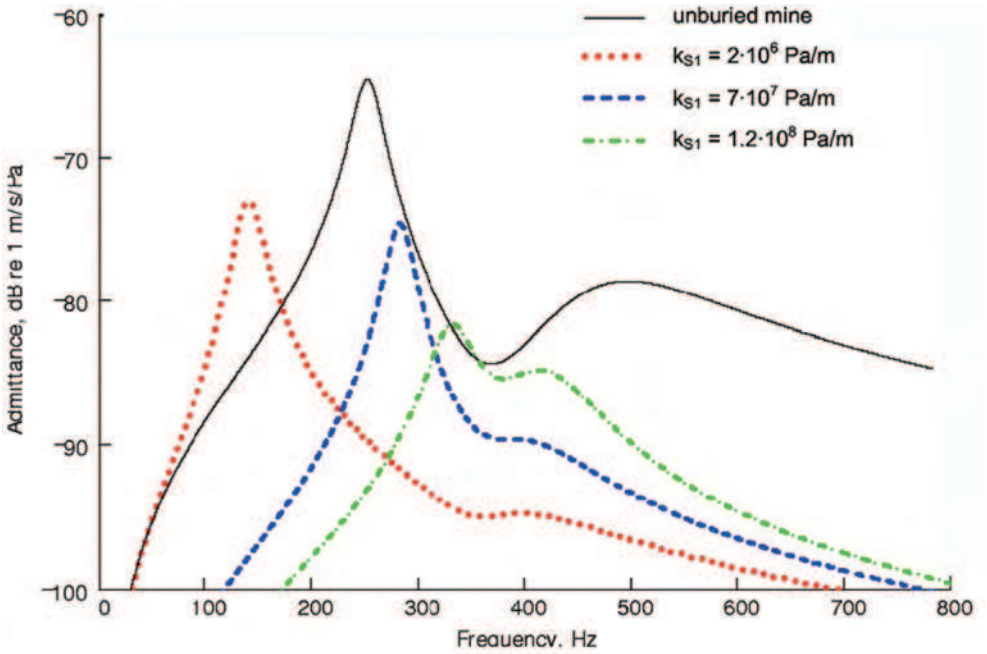

Fig. 10. Calculated admittances of the AT mine VS-1.6 illustrating the reduction of the vibration amplitude due to soil shear stiffening (Zagrai, et.al., 2005)

The soil column shear stiffness variations could be caused by different factors such as grain size distribution, compaction, consolidation, vegetation, freezing, moisture content, etc. Mine burial depth is also a significant factor affecting the total shear stiffness of the soil column above a mine, as shown in Zagrai, et al., 2005.

4.2 Effect of Burial Depth on the Soil-mine Resonance Frequency

The maximum detection contrast for most mines coincides with the first resonance of the coupled soil-mine system, as followed from the solution (6) in which soil parameters are depth-dependent. Using the depth dependencies defined by formulas (3) and (5) it can be shown that the increase in the burial depth, H, leads to downward resonance frequency shift along with the reduction of the contrast. However, experimental investigations, Sabatier, et.al., 2002, Fenneman, et.al ., 2003, Zagrai, et.al., 2004, revealed that at certain depths the soil-mine system resonance exhibits an unexpected upward frequency shift suggesting a more complex dependence of soil parameters with depth.

Fig.11 demonstrates soil-mine resonance frequency dependence on the burial depth, Zagrai, et.al. 2004. Here the resonance frequency decreases initially and then, at a certain burial depth, it starts to increase.

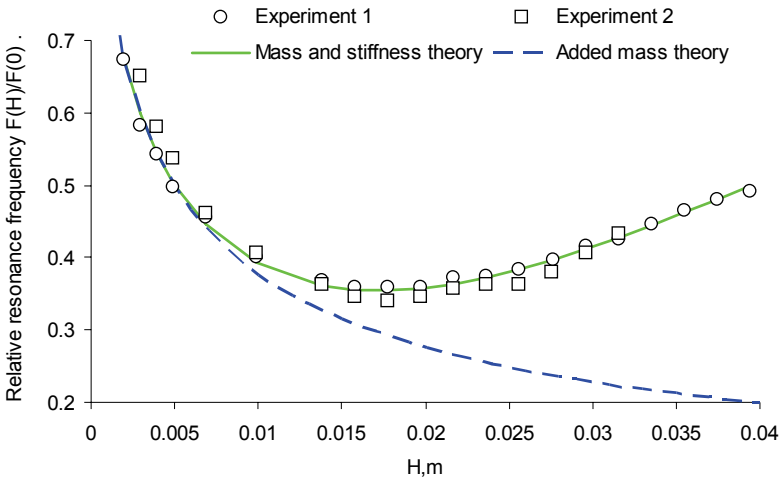

Fig. 11. Soil-mine relative resonance frequency versus burial depth, H. The relative frequency is a ratio between the resonance frequency at particular burial depth and the resonance frequency of the flush-buried mine, i.e. at zero depth

The downward shift of the resonance frequency with increase of the burial depth can be explained by the added mass of soil column (dashed line). However, the upward shift at greater depths needs an additional explanation.

The resonance frequency increase indicates that the system is stiffening with depth. We considered two possible explanations of this phenomenon. The first one deals with stiffening of the mine casing due to nonlinear stress-strain relationship for the casing. In other words, an additional soil load modifies stiffness of the casing and, respectively, stiffness of the whole soil-mine system. This explanation, however, could only hold for exceedingly high stresses which unlikely to occur under given experimental conditions. To estimate the effect of casing stiffening due to some additional mass, we conducted an experiment in which concentrated weights were placed on the casing and the impedance frequency response was measured using non-contact LDV and a microphone. The test revealed only the decrease of the resonance frequency consistent with the added mass effect. Therefore, we suggest that the upward frequency shift is due to increase of the soil shear stiffness, as elaborated by Zagrai, et al, 2005. According to this study, $K_{S1} \sim H^3$ rather than H, as was initially prescribed by Eq.(5).

4.3 Effect of Soil Moisture

Soil moisture content variation is a common factor in open fields. It was observed that vibrations of a mine buried in wet or dry soil could be considerably different. Fig.12 demonstrates vibration responses measured above a mine buried in wet and dry sand. In this test the mine initially was buried in wet sand and than the sand naturally dried, so the dry sand response was measured for the same undisturbed soil-mine setup. These

measurements show that the soil moisture has a pronounced effect: it shifts the resonance frequency and changes the resonance amplitude, effectively changing the detection contrast.

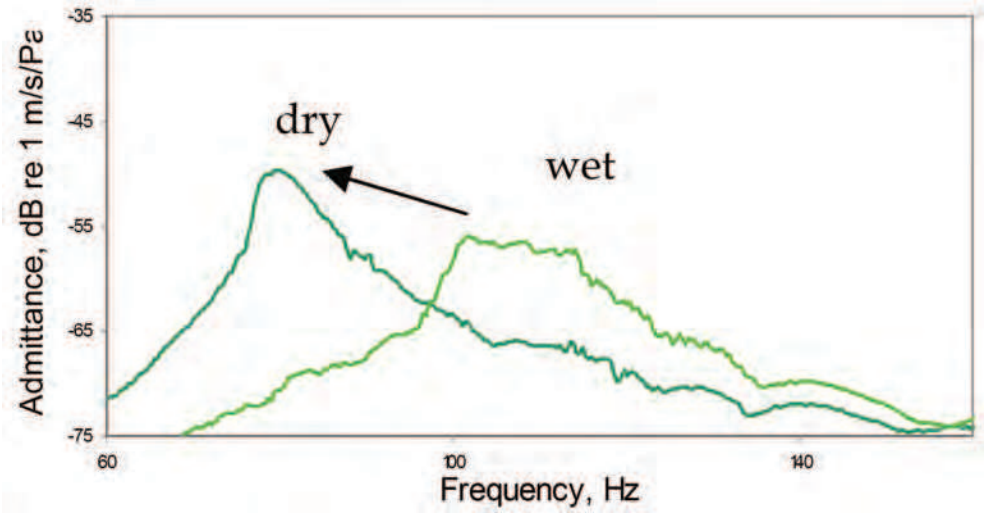

Fig.12. Effect of soil moisture on the resonance vibration of mine simulant buried at 25 mm

In order to understand and quantify the moisture effect, we conducted a laboratory test in which the plastic mine simulant was buried under gradually increasing sand depths subjected to the controlled level of water saturation. The soil water content, WC, was calculated utilizing a gravimetric method as following:

$WC=W_{water}/(W_{soil}+W_{water})\cdot 100\%$,

where W_{soil} and W_{water} are respective weights of the soil and water. Initially, we repeated the experiment with the layers of dry sand similar to described in the previous section. A relative frequency shift of the resonance frequency $F(WC=0\%)/F_0$ (here F_0 is the resonance frequency of flush-buried mine) due to increasing burial depths, H, was measured and result is presented in Fig. 13 with solid dots line. Then, the test was repeated for different moisture contents ranging from 2.5% to 15%. Moisture was uniformly distributed throughout the sand column and was kept constant for each test run. Experimental results depicted in Fig. 13 show that moisture significantly affects the dynamic resonance of the buried mine, especially at the greater depths.

It is interesting to note that the significant upward frequency shift occurs for the relatively small moisture content, and does not change for the higher moisture levels. This observation coupled with our previous conclusion that the upward frequency shift is due to soil shear stiffness increase, lead us to believe that the introduction of moisture results in soil consolidation. Consolidated soil has appreciably higher shear stiffness. As the test reveals, even relatively small water content creates appreciable consolidation (stiffening) effect shifting the resonance frequency upward and reducing the vibration velocity (Fig.12). Further increase of the water content adds little to already consolidated soil resulting in an insignificant frequency shift. These effects were recently confirmed by Horoshenkov & Mohamed, (2006).

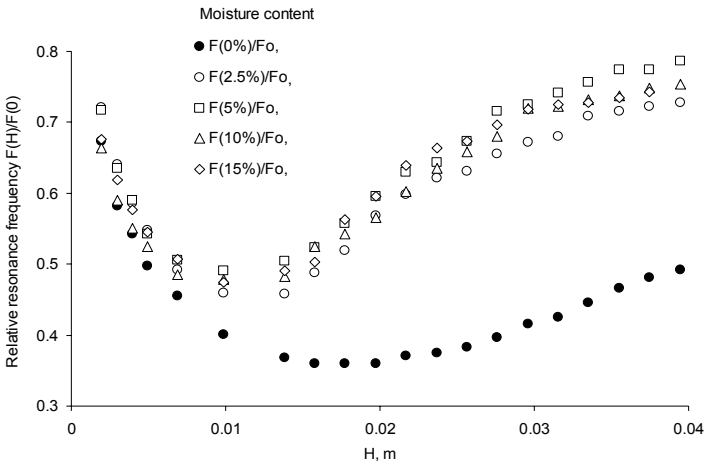

Fig.13. Effect of moisture and burial depth on soil-mine resonance frequency

5. Nonlinear Dynamics of Soil-mine System

Along with the resonance dynamics, buried mines exhibit highly nonlinear behavior, amplified by the resonance. If the system is excited by two harmonic signals, the nonlinearity manifests itself through generation of the nonlinear frequencies: harmonics, combination, and intermodulation frequencies, as depicted in Fig.14. The nonlinear frequencies were successfully employed for the detection of buried landmines (Donskoy, 1998 and the following publications). The detection scheme is similar to that shown in Fig.1. Here the acoustic or seismic waves contain two frequencies swept across the frequency band, typically 50 – 500 Hz. Scanning LDV measures the response at the nonlinear frequencies outputting the nonlinear vibration image of the buried mine. Among the advantages of the nonlinear detection approach are high detection contrast and low false alarm rate even for small plastic AP mines.

We believe that the major reason for the strong nonlinearity is the lack of bonding at the soil-mine interface. The stress-strain dependence at the interface is quite different during the compressive and tensile phases of vibration: under tensile stress, separation of soil grains may occur at the soil-mine interface whereas under compressive stress a mine and the soil are always in contact. This asymmetric response leads to noticeable nonlinear effects such as the generation of harmonics and signals with combination and intermodulation frequencies.

There are two possible mechanisms for separation at the interface. In the first one, the level of applied vibrational force (stress) is higher than the weight of the soil column. In this case, the soil will "jump or bounce" on the top of the mine leading to a very strong nonlinearity. This mechanism, however, should occur rarely considering the practical levels of vibrational excitation. Indeed, in most of the field tests we conducted, the soil surface acceleration was below the gravitational acceleration implying that the vibrational force was smaller than the

weight of the soil above the mine. Nevertheless, noticeable nonlinear effects were still observed suggesting that there should be another mechanism of "separation".

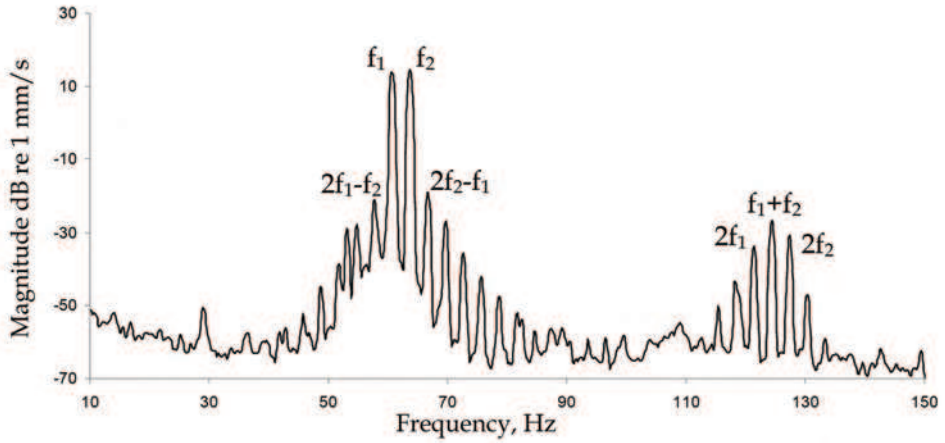

Fig. 14. Vibration spectrum measured above buried in sand plastic mine simulant. Here f_1 & f_2 are the fundamental (excitation) frequencies and f_1+f_2 , $2f_{1,2}$, $2f_2-f_1$, $2f_1-f_2$ are the nonlinear (sum, harmonic, and intermodulation) frequencies

Since both soil and mine are mechanical systems, each with their own inertia and stiffness, their respective phases of oscillation depend on the relative contributions of inertia and stiffness. If stiffness is the dominant contributor to the system's mechanical impedance, then the system will oscillate in phase with the applied external force. At higher frequencies, however, the inertial contribution becomes dominant and the system oscillates in the opposite phase with respect to the external force. Therefore, the mine and soil may oscillate with the opposite phases depending on relative values of their mechanical impedances. This leads to the soil separation at the interface. When this mechanism is dominant, the separation is taken place even at relatively low levels of the exerted dynamic force.
In addition to the interface nonlinearity, soil itself can contribute to the overall nonlinear dynamics of the soil-mine system, as suggested by Korman & Sabatier, 2004. However, in the foregoing discussion, we will focus only on the interface nonlinearity, following Donskoy, et al., 2004.

5.1 Nonlinear lump-element model of soil-mine system

The interface nonlinearity can be described using a generic form of Hooke's law:

$$P_m = \xi \cdot \left(K_m + K_m^{nl}(\xi)\right), \tag{7}$$

where ξ is the deformation, K_m is the mine linear stiffness coefficient, $K_m^{nl}(\xi)$ describes the nonlinear stiffness at mine interface, and P_m is the normal stress (pressure) applied to the interface. Accounting for the introduced nonlinear stiffness, the mechanical mass-spring-